Structure, characterization and DFT studies of 1,2- Dichloro-4-fluoro-5-Nitrobenzene

S. Seshadri*[1], M. Padmavathy[2]

[1]Head & Associate professor in PG & Research Department of Physics, Urumu Dhanalakshmi College, Trichy, India

[2]Department of Physics, Shrimati Indira Gandhi College, Trichy, India

ABSTRACT

The 1,2-Dichloro-4-fluoro-5-Nitrobenzene (DFNB) subjected to density functional theory (DFT) studies using B3LYP/6-31+G(d,p) method. Characterization was done by FT-IR, FT-Raman and NMR (13C and 1H) spectroscopic techniques. Molecular electrostatic potential (MEP) study was also determined.

Keywords : DFT, FT-IR, FT-Raman, NMR, MEP.

I. INTRODUCTION

Nitrobenzene very poisonous, flammable, pale yellow and liquid aromatic compound with an odor like that of bitter almonds. It is sometimes called oil of mirbane or nitrobenzol. Nitrobenzene melts at 5.85℃, boils at 210.9℃ is only slightly soluble in water but is very soluble in ethanol, ether and benzene. Nitrobenzene is prepared by treating benzene with a mixture of nitric and sulfuric acid in the resulting nitration reaction one hydrogen in the benzene molecule is replaced with a nitro group.

The major use of nitrobenzene is in the production of aniline, commercially the most important amine. Nitrobenzene is heated with iron and dilute hydrochloric acid and the resulting anilinium chloride is treated with sodium carbonate to release aniline. In the pharmaceutical industry nitrobenzene is used in the production of the analgesic acetaminophen or paracetamol. Nitrobenzene is also used in shoe and floor polishes, leather dressings and paint solvents to mask unpleasant odors. As oil of mirbane, nitrobenzene was used as an inexpensive perfume for soaps and cosmetics but is now considered too toxic for such applications.

The compound 1,2-Dichloro-4-fluoro-5-Nitrobenzene (DFNB) is used as a reagent for the detection and determination of nicotinic acid, nicotinamide and other pyridine compounds. It is also used in the manufacture of azo dyes, fungicides, rubber chemicals and explosives and as an algicide in coolant water of air conditioning systems. Contact sensitizations with DFNB have been used as a measure of cellular immunity.

Various spectroscopic studies of halogen and nitrogen substituted benzene compounds have been reported in the literature [1–5]. DFNB belongs to the group of organic halogen compounds replacing two hydrogen atoms in benzene by methyl (CH_3) and a nitro group (NO_2). Literature survey reveals that no detailed B3LYP with 6-31+G(d,p) basis set of FT-IR, FT-Raman and NMR (^{13}C and ^{1}H) chemical shifts calculation of DFNB have been reported so far. It is, therefore thought worth to make this theoretical and experimental vibrational spectroscopic research based on molecular structure to give the correct assignment of fundamental bands in the experimentally observed FT-IR and FT-Raman spectra. In this study, molecular geometry and vibrational frequencies are calculated using hybrid density functional method. This method

predicts relatively accurate molecular structure and vibrational spectra with moderate computational effort.

II. EXPERIMENTAL DETAILS

The fine sample of 1,2-Dichloro-4-fluoro-5-Nitrobenzene (DFNB) is purchased from Sigma-Aldrich chemicals, USA and it was used as such without any further purification. The FT-IR spectrum of the compound has been recorded in Perkin-Elimer 180 spectrometer in the range of 4000–400 cm^{-1}. The spectral resolution is ±2 cm^{-1}. The FT-Raman spectrum of the compound was also recorded in same instrument with FRA 106 Raman module equipped with Nd:YAG laser source operating in the region 3500–100 cm^{-1} at 1064 nm line width with 200 Mw powers. ^{13}C and ^{1}H NMR spectra were taken in CDCl$_3$ solutions and all signals were referenced to TMS on a BRUKER TPX-400 FT-NMR spectrometer.

III. COMPUTATIONAL DETAILS

The molecular structure of the DFNB molecule in the ground state is computed by B3LYP/6-31+G(d,p) method. The optimized structural parameters are used in the vibrational frequency calculations at B3LYP level. The DFT calculations were carried out for DFNB with GAUSSIAN 09W program package [6]. Initial geometry generated from the standard geometrical parameters was minimized without any constraint, which invokes Becke's three parameter hybrid method [7] with Lee-Yang-Parr correlation functional (LYP) [8], implemented with the same basis set for better description of the bonding properties. All the parameters were allowed to relax and all the calculations converged to an optimized geometry which corresponds to a true minimum, as revealed by the lack of imaginary values in the wave number calculations. The Cartesian representation of the theoretical force constants have been computed at the fully optimized geometry.

The multiple scaling of the force constants were performed according to scaled quantum mechanical (SQM) procedure [9] using linear scaling in the natural internal coordinate representation [10]. Transformation of force field, the subsequent normal coordinate analysis (NCA) including the least square refinement of the scale factors and calculation of the total energy distribution (TED) were done on a PC with the MOLVIB program (version V7.0-G77) written by Sundius [11,12].The calculated frequencies are scaled by 0.9689 scale factor [13, 14]. As a result, the unscaled frequencies, reduced masses, force constants, infrared intensities and Raman activities were obtained. The systematic comparison of the results from DFT theory with results of experiments has shown that the method using B3LYP functional is the most promising in providing correct vibrational wave numbers.

The Raman activities (S_i) calculated by the Gaussian 09W program was converted to relative Raman intensities (I_i) using the following relationship derived from the intensity theory of Raman scattering [15, 16].

$$I_i = \frac{f(v_0 - v_i)^4 S_i}{v_i[1 - \exp(-hc v_i / KT)]}$$

(1)

where v_0 is the laser exciting wavenumber in cm^{-1} (in this work, we have used the excitation wavenumber v_0 = 9398.5 cm^{-1}, which corresponds to the wavelength of 1064 nm of a Nd:YAG laser), v_i is the vibrational wavenumber of the ith normal mode (cm^{-1}), while S_i is the Raman scattering activity of the normal mode v_i, f (is a constant equal to 10^{-12}) is a suitably chosen common normalization factor for all peak intensities h, k, c and T are Planck and Boltzmann constants, speed of light and temperature in Kelvin, respectively.

In this study, the ^{13}C and ^{1}H NMR chemical shifts and nuclear magnetic shielding tensor values of DFNB in the ground state for B3LYP/6-31+G(d,p) method were

calculated with the gauge independent atomic orbital (GIAO) method [17, 18]. All calculations were performed using Gaussian 09W program package [9] employing B3LYP method with 6-31+G(d,p) basis set.

Molecular electrostatic potential (MEP) is related to the electronic density and is considered as a fundamental determinant of atomic and molecular properties. Therefore, MEP has largely been used as a molecular descriptor of the chemical reactivity of a number of biological systems, which take part in both electrophilic and nucleophilic reactions as well as hydrogen bonding interaction [19, 20]. MEP, $V(\vec{r})$ at a given point r(x, y, z) in the vicinity of a molecule is defined in terms of the interaction energy between the electrical charge generated from the molecular electrons, nuclei and a positive test charge (a proton) located at $\vec{r}$. For the systems studied the MEP values were calculated as described previously using the equation [21].

$$V(\vec{r}) = \sum_A \frac{Z_A}{|\vec{R} - \vec{r}|} - \int \frac{\rho(\vec{r}')dr'}{|\vec{r}' - \vec{r}|}$$

(2)

where $\rho(\vec{r}')$ is the electron density function of the molecule, Z_A is the charge of nucleus A located at $\vec{R}_A$ and r' is the dummy integration variable.

For investigating molecular electrostatic potential (MEP) surface are plotted over the optimized electronic structures of DFNB using density functional B3LYP method with 6-31+G(d,p) basis set. Because the computationally or experimentally observed MEP surface is directly provide information about the electrophilic (electronegative charge region) and nucleophilic (most positive charge region) regions. Figs. 5 and 6 show the computationally observed MEP contour map with the fitting point charges to the electrostatic potential $V(\vec{r})$ for title molecule. The electrostatic potential $V(\vec{r})$ at any point in space around a molecule by charge distribution is given by equation 2.

IV. RESULTS AND DISCUSSION

4.1. Vibrational assignments

The labelling of atoms of DFNB is shown in Figure 1. The molecule contains two Cl and a NO2 group connected with benzene ring. Experimental and simulated spectra of FT-IR and FT-Raman are presented in Figs. 2 and 3, respectively.

The DFNB molecule consists of 14 atoms, which undergoes 36 normal modes of vibrations. On the assumption of C1 group of symmetry, the numbers of vibration modes of the 36 fundamental vibrations of the molecule are distributed as 25 in-plane and 11 out-of-plane vibrations of same symmetry species.

The vibrational frequencies calculated at B3LYP level are scaled by 0.905 [22] and the range of wave numbers above 1700 cm^{-1} are scaled as 0.958 and below 1700 cm^{-1} scaled as 0.983 for title compound. After scaled with the scaling factor, the deviation from the experiments is less than 10 cm^{-1} with a few exceptions. The force fields determined were used to calculate the vibrational total energy distribution (TED) among the normal coordinates. Finally, the TED for each normal mode among the symmetry coordinates is calculated and given in Table 1.
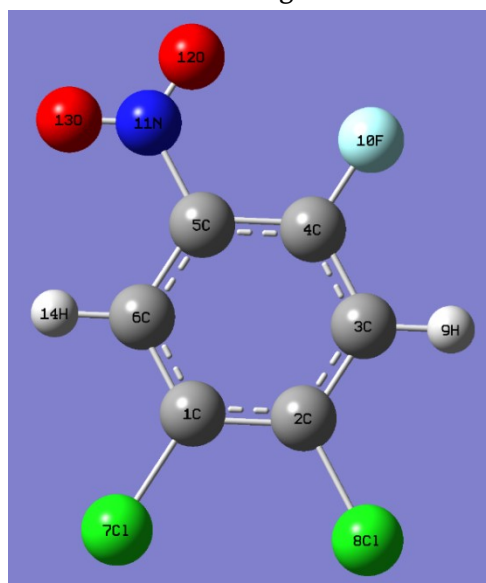

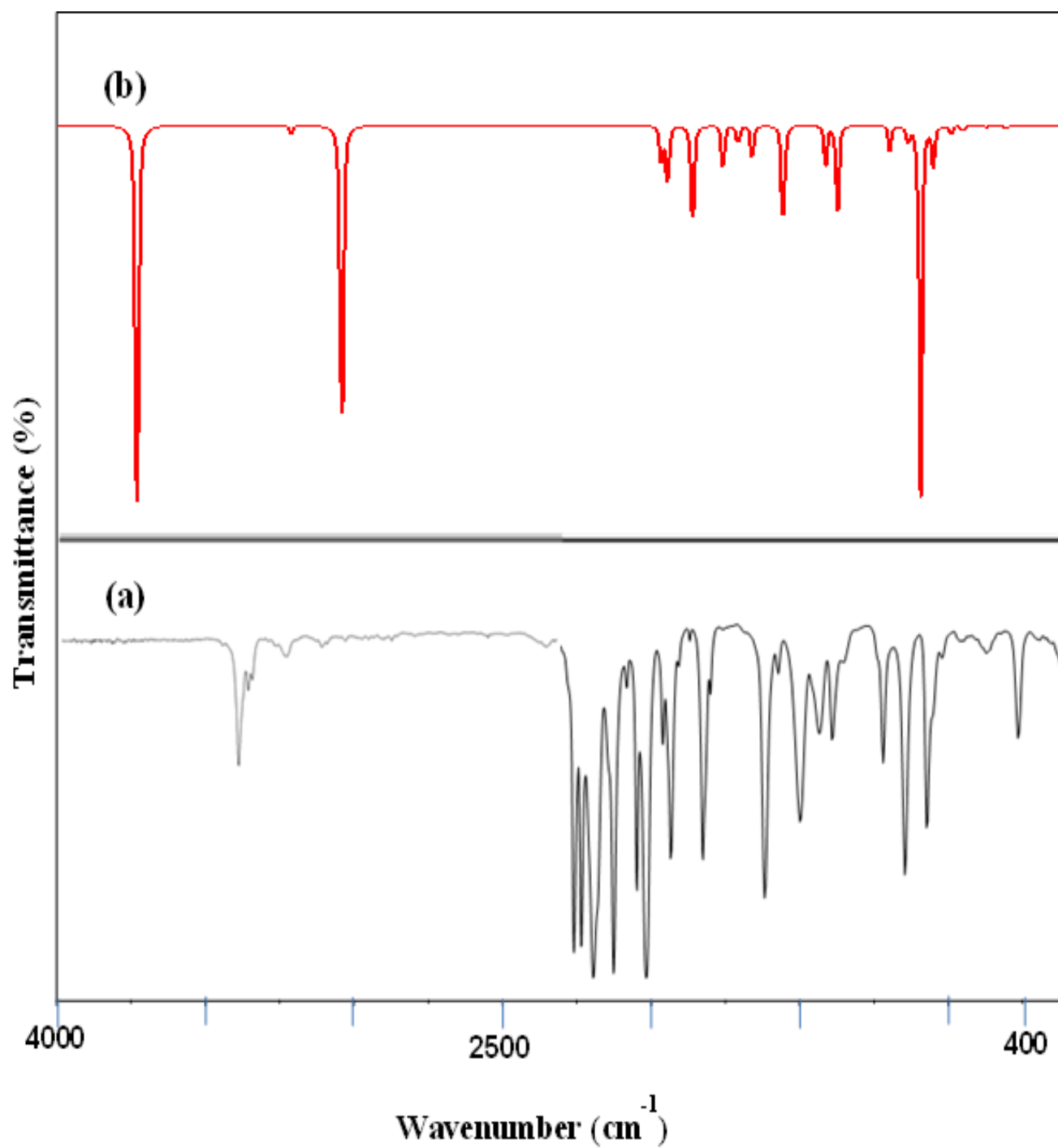**Figure 1.** Atoms with labelling of DFNB.

Figure 2. Comparison of (a) experimental and (b) calculated spectra of DFNB.
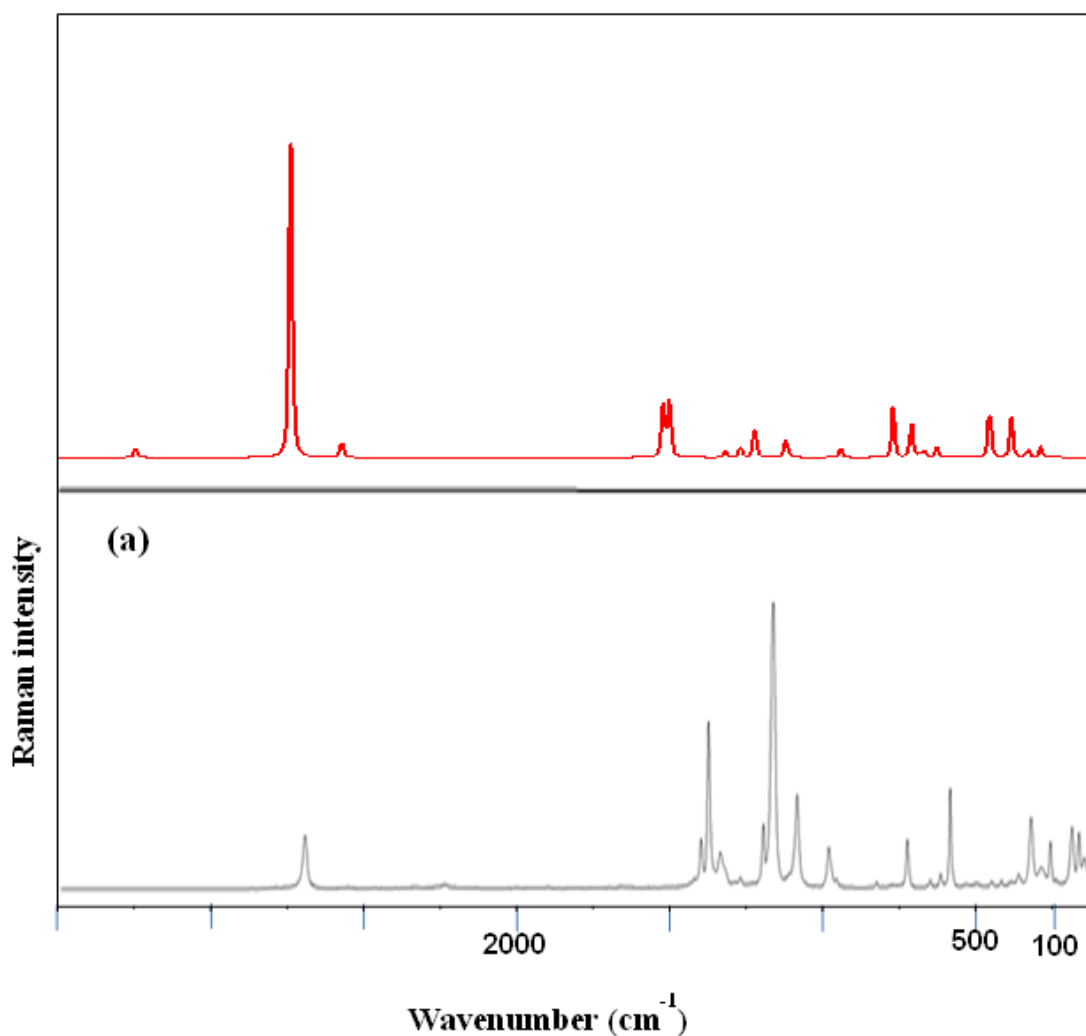
Figure 3. Comparison of (a) experimental and (b) calculated spectra of DFNB.

Table 1. The observed FT-IR, FT-Raman and theoretically calculated frequencies by B3LYP/6-31+G(d,p) method along with their assignments, IR intensities (Km mol^{-1}) and Raman intensities (Å^4 amu^{-1}) of DFNB.

No.	Observed wavenumbers (cm^{-1})		Calculated wavenumbers (cm^{-1})		IR Intensities	Raman intensities	Vibrational assignments
	FT-IR	FT-Raman	Unscaled	Scaled			
1	3300(m)		3260	3175	14.63	55.47	νCH(98)
2	3250(vw)		3249	3127	4.27	81.33	νCH(97)
3	1800(s)		1709	1693	246.38	11.80	NO2asym(98)
4		1600(vw)	1658	1584	78.21	64.62	NO2sym(95)
5	1625(s)		1625	1544	33.83	60.61	νCC(92)
6	1500(m)		1518	1485	186.57	1.01	νCC(89)
7	1425(w)	1425(vw)	1425	1401	111.02	61.16	νCC(88)
8	1360(w)	1400(s)	1413	1396	213.22	143.64	νCC(84)
9		1311(w)	1349	1318	26.14	3.46	νCC(82)
10			1309	1285	72.77	47.12	νCC(81)
11	1250(m)	1260(vw)	1241	1202	2.99	0.92	βCH(71)
12		1170(vw)	1168	1121	92.84	39.45	βCH(75)
13	1100(s)	1150(vs)	1125	1104	4.25	2.76	νCF(65)
14	1060(m)	970(m)	975	956	80.32	1.92	νCN(61)
15			930	905	23.21	1.01	γCH(56)

16			864	845	17.01	3.04	vCCl(60)
17		800(vw)	863	831	18.35	7.78	vCCl(52)
18			764	712	12.59	1.84	NO2rock(54)
19		740(m)	734	711	38.22	1.74	γCH(51)
20			694	654	29.59	9.91	NO2sciss(59)
21		630(vw)	664	633	0.01	0.23	βCCl(52)
22			619	592	1.08	0.37	βCN(51)
23		610(vw)	611	574	2.42	1.96	βCCl(51)
24		500(vw)	537	512	9.59	0.76	NO2wagg(43)
25			457	421	2.44	0.02	Rtrigd(42)
26	400(m)		429	405	0.35	3.47	tRtrigd(36)
27			377	345	0.65	8.07	Rasymd (37)
28		360(vw)	368	322	3.24	0.69	γCN(33)
29			313	297	0.38	3.05	βCF(31)
30		250(vw)	299	263	0.38	0.27	γCCl(52)
31			224	214	0.16	1.83	Rsymd (37)
32		200(m)	203	183	0.35	1.64	γCCl(41)
33			186	147	1.33	0.50	NO2twist(41)
34		140(vw)	143	121	2.47	0.26	tRasymd (37)
35			70	61	0.75	0.05	tRsymd (37)
36			52	45	0.07	0.68	γCF(31)

Experimental relative intensities are abbreviated as follows: vs-very strong, s-strong, m-medium, w-weak, vw-very weak. Abbreviations; ν-stretching, sym-symmetric stretching, asym-asymmetric stretching, β-in-plane bending, γ-out-of-plane bending, d-deformation, R-ring, trig-trigonal, sciss-scissoring, rock-rocking, wagg-wagging, twist-twisting.

4.1.1. C–H vibrations

Aromatic compounds commonly exhibit multiple bands in the region 3100–3000 cm⁻¹ due to C–H stretching vibration [23]. It has been argued that in p-anisaldehyde the, the FT-IR bands observed at 3186 and 3092 cm⁻¹ have been assigned to C–H stretching vibration. The FT-IR bands observed at 3300(m), 3250(vw) cm⁻¹ in DFNB were assigned to C–H stretching modes.

In benzene like molecule C–H in-plane bending vibrations interact with C–C stretching vibrations and are observed as a number of bands in the region 1000–1300 cm⁻¹ [23, 24]. The FT-IR band identified at 1250(m) cm⁻¹ and FT-Raman band at 1260(vw), 1170(vw) cm⁻¹ were assigned to C–H in-plane bending vibration of DFNB.

The C–H out-of-plane bending vibrations occur in the region 900–667 cm⁻¹ [24]. The bands observed at 740(m) cm⁻¹ in FT-Raman spectrum of DFNB. The theoretically calculated values for C–H vibrational modes by B3LYP/6-31+G(d,p) method gives good agreement with experimental data.

4.1.2. Ring Vibrations

Most of the ring vibrational modes are affected by the substitutions of functional groups. The characteristic ring stretching vibrations are assigned in the region 1650–1300 cm⁻¹ [25]. Therefore, the C–C stretching vibrations of DFNB are found at 1625(s), 1500(m), 1425(w), 1360(w) in FT-IR spectrum and 1425(vw), 1400(s), 1311(w) in FT-Raman spectrum for DFNB. The theoretically computed values for C–C vibrational modes by B3LYP/6-31+G(d,p) method gives excellent agreement with experimental data. Small changes in wavenumber observed for these modes are due to the changes in force constant/reduced mass, resulting mainly due to addition of fluorine group to nitro.

4.1.3. C–Cl vibrations

The vibrations belonging to the bond between the ring and the halogen atoms are worth to discuss here, since mixing of vibrations is possible due to the presence of heavy atoms on the periphery of the title molecule [26]. In DFNB, the C–Cl stretching vibrations appeared at 800(vw) cm^{-1} in FT-Raman spectrum. The C–Cl in-plane bending vibrations were found at 630(vw) and 610(vw) cm^{-1} in FT-Raman spectrum. The C–Cl out-of-plane bending mode is recorded at 250(vw) and 200(m) cm^{-1} in FT-Raman spectrum. The calculated values of C–Cl stretching, in-plane and out-of-plane bending modes are found to be at 845, 831, 633, 574, 263 and 183 cm^{-1} in B3LYP/6-31+G(d,p).

4.1.4. Nitro group vibrations

Aromatic nitro compounds have strong absorptions due to asymmetric and symmetric stretching vibrations of the nitro group at 1570–1485 and 1370–1320 cm^{-1}, respectively, Hydrogen bonding has a little effect on the nitro group asymmetric stretching vibrations [27, 28]. The strong and very weak bands at 1800 cm^{-1} and 1600 cm^{-1} have been assigned to asymmetric and symmetric stretching modes of nitro group. Aromatic nitro compounds have a band of weak to medium intensity in the region 590–500 cm^{-1} [29] due to the out-of-plane bending deformations mode of nitro group. This is observed at 500 cm^{-1} in FT-Raman spectrum. The in-plane nitro group deformations vibrations have a week to medium absorption in the region 775–660 cm^{-1} [30, 31]. In DFNB, the nitro group deformation is found within the characteristics region.

4.1.5. C–N vibrations

The C–N stretching and C–N bending vibrations of a nitro group occur near 870 and 610 cm^{-1}, respectively [32]. The bands are assigned to C–N stretching vibration of a nitro group for DFNB have been found at 1060(m) and 970(m) cm^{-1}. The C–N out-of-plane bending vibrations are occurred within the characteristics region. From these observations it is found that the stretching bond; C–N is influenced by other modes. After scaling down, the computed value for C–N stretching vibration by B3LYP/6-31+G(d,p) methods nearly coincide with observed values of FT-IR and FT-Raman and these assignments are in good agreement with the literature data.

5. NMR Spectral Analysis

The theoretical ^{13}C and ^{1}H NMR chemical shifts of C and H are compared with the experimental data [33] as shown in Table 2. Chemical shifts are reported in ppm for ^{13}C and ^{1}H NMR spectra [34]. According to the Figs. 4(a) and 4(b), the geometry optimization of the title molecule is calculated with B3LYP/6-31+G(d,p) basis set. Then, gauge independent atomic orbital (GIAO) ^{13}C and ^{1}H chemical shift calculations are performed by the same basis set using CDCl3 solvent. Usually the experimental NMR spectra, the benzene carbons are overlapping with chemical shift values from 60–20 and for hydrogen chemical shift 1.55–0.88 ppm [33, 35]. The experimental and calculated ^{13}C and ^{1}H NMR isotropic chemical shifts (ppm) of DFNB is shown in Figure 4.

In the present study, the experimental chemical shift values of DFNB carbons are in the range of 158–79 ppm. From the plotted ^{13}C NMR spectra it is found that, the title molecule ring carbon atoms C4 and C6 have more chemical shift compared with substitutional carbon atoms due to conjugation of F, Cl and nitro groups. C1 and C3 atoms has least chemical shift (79 and 122 ppm) compared with other carbon atoms, due to the increasing deshielding effect and more electronegative charge of that atom.

The chemical shift for ^{1}H atoms of DFNB are falls in the range of 8.4 and 7.5 ppm. Some chemical shifts are slightly low because the hydrogen atoms are bonded or nearby with the acceptor atom or group which decreases the chemical shift of ^{1}H atom. H9 atom had chemical shift is very high, this is due to the ring in which the replacing H with C (more electronegative)

deshields C to which it is attached. All computations are in good agreement with experimental data.

Table 2. Experimental and theoretical ^{13}C and ^{1}H chemical shift (ppm) of DFNB.

Atoms	Theoretical Shift (ppm)	Experimental Shift (ppm)
C1	81	79
C2	139	133
C3	125	122
C4	154	156
C5	136	142
C6	162	158
H8	7.56	7.5
H9	7.87	8.4
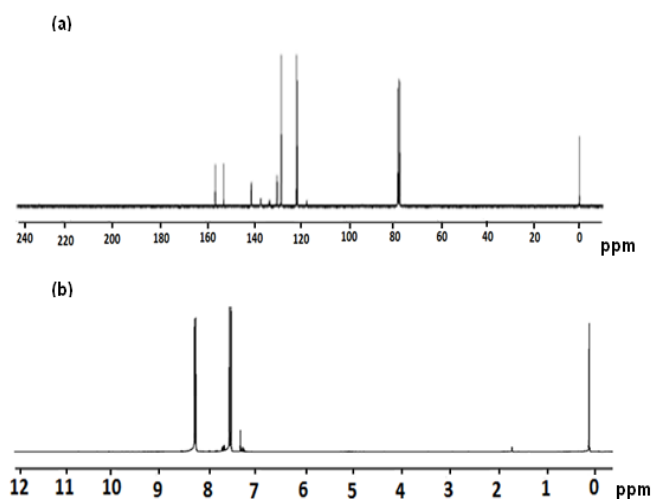
Figure 4. The experimental (a) ^{13}C and (b) ^{1}H NMR spectra of DFNB.

V. MOLECULAR ELECTROSTATIC POTENTIAL (MESP) ANALYSIS

The total electron density and MESP surfaces of the DFNB molecule under investigation are constructed by using B3LYP/6-31+G(d,p) method. Molecular electrostatic potential (MESP) mapping is very useful in the investigation of the molecular structure with its physiochemical property relationships [36]. The total electron density mapped with electrostatic potential surface, the contour map of electrostatic potential and molecular electrostatic potential surface of DFNB are shown in Figure 5 and 6.

The colour scheme for the MESP surface is red-electron rich, partially negative charge; blue-electron deficient, partially positive charge; light blue-slightly electron deficient region; yellow-slightly electron rich region; green-neutral; respectively. The Figs. 5 and 6 indicates that the region around oxygen and nitrogen atoms represents the most negative potential region (red). The predominance of light green region in the MESP surfaces corresponds to a potential halfway between the two extremes red and dark blue colour. The isosurface clearly reveals the presence of high positive charge on the nitrogen atom.
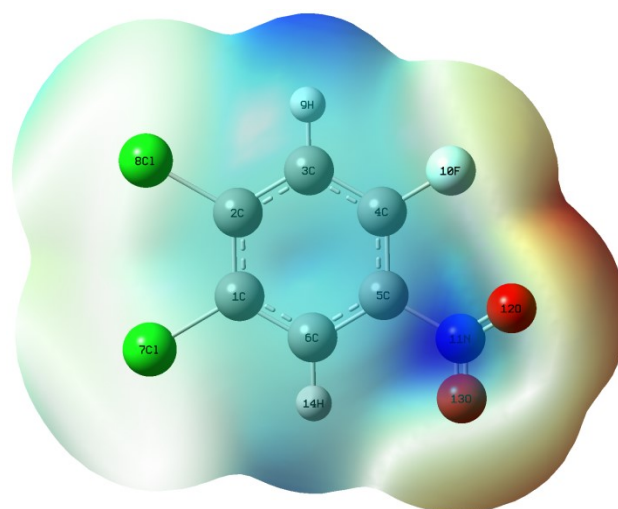

Figure 5. The total electron density mapped with electrostatic potential surface of DFNB.
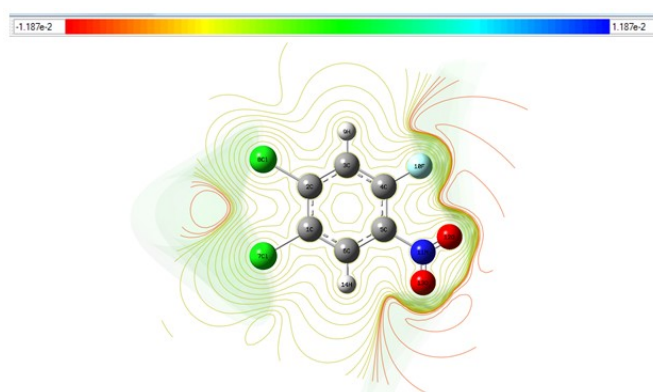

Figure 6. The contour map of electrostatic potential of DFNB.

VI. CONCLUSION

The vibrational frequencies of the fundamental modes of the DFNB have been precisely assigned and analyzed and the theoretical results were compared with the experimental vibrations. The observed and calculated fundamental frequencies by B3LYP method using 6- 31+G(d,p) basis set shows similar profiles in both position and intensities making normal mode assignments with confidence. ^{1}H and ^{13}C NMR spectra were recorded and the ^{1}H and ^{13}C NMR isotropic chemical shifts were calculated. The assignments made were compared with the experimental values. The MEP map shows the negative potential sites are on chlorine atom as well as the positive potential sites are around the hydrogen atoms.

VII. REFERENCES

[1]. V. Suryanarayana, A. Pavan Kumar, G. Ramana Rao, G.C. Pandey, Spectrochim. Acta 48A 1992: 1481.

[2]. V. Krishnakumar, N. Jayamani, R. Mathammal, J. Raman Spectros. 40 2009: 936.

[3]. P. Muralidhar Rao, G. Ramana Rao, J. Raman Spectros. 20 1989: 529.

[4]. J. Clarkson, W. Ewen Smith, J. Mol. Struct. 655 2003: 413.

[5]. D.K. Singh, S.K. Srivastava, B.P. Asthana, Vib. Spectros, 56 2011: 26.

[6]. M.J. Frisch, A.B. Nielsen, A.J. Holder, Gaussview user's manual, Gaussian Inc., Pittsburgh, PA, 2009.

[7]. A.D. Becke, J. Chem. Phys. 98 1993: 5648.

[8]. C. Lee, W. Yang, R.C. Parr, Phys. Rev. B 37 1998: 785.

[9]. P. Pulay, G. Fogarasi, G. Pongor, J.E. Boggs, A. Vargha, J. Am. Chem. Soc. 105 1983: 7037.

[10]. G. Fogarasi, P. Pulay, in: Durig J. R. (Ed.) Vibrational Spectra and Structure, Vol.14, Elsevier, Amsterdam, Chapter 3, 1985: 125.

[11]. T. Sundius, Vib. Spectrosc. 29 2002: 89.

[12]. MOLVIB (V.7.0): Calculation of Harmonic Force Fields and Vibrational Modes of Molecules, QCPE Program No. 807, 2002.

[13]. D.C. Young, Computational Chemistry: A Practical guide for applying Techniques to Real world Problems (Electronic), John Wiley and Sons Inc., New York, 2001.

[14]. N. Sundaraganesan, S. IIlakiamani, H. Saleem, P.M. Wojciechowski, D. Michalska, Spectrochim. Acta 61A 2005: 2995.

[15]. G. Keresztury, J.M. Chalmers, P.R. Griffiths (Eds.), Raman Spectroscopy: Theory in Hand Book of Vibrational Spectroscopy, John Wiley & Sons Ltd., New York, 1 2002.

[16]. G. Keresztury, S. Holly, G. Besenyei, J. Varga, A.Y. Wang, J.R. Durig, Spectrochim. Acta A, 49 1993: 2007.

[17]. M. Karabacak, D. Karagoz, M. Kurt, Spectrochim. Acta 61A 2009: 2995.

[18]. N. Sundaraganesan, S. Kalaichelvan, C. Meganathan, B. Dominic Joshua, J. Cornard, Spectrochim. Acta 71A 2008: 898.

[19]. C. Muñoz-Caro, A. Niño, M.L. Senent, J.M. Leal, S. Ibeas, J. Org. Chem. 65 2000: 405-410.

[20]. S. Miertus, E. Scrocco, J. Tomasi, Theor. Chem. Acc. 103 2000: 343-345.

[21]. P. Politzer, J. Murray, Theor. Chem. Acc. 108 2002: 134-142.

[22]. D.C. Young, Computational Chemistry: A Practical Guide for Applying Techniques to RealWorld Problems (Electronic), John Wiley & Sons Inc., New York, 2001.

[23]. G. Socrates, Infrared and Raman Characteristic Group Frequencies Tables and Charts, third ed., John Wiley and Sons, Chichester, 2001.

[24]. J. Mohan, Organic Spectroscopy, Principles and Applications, second ed., New Age International Private Limited Publishers, New Delhi, 2001.

[25]. K. Parimala, V. Balachandran, Spectrochim. Acta 81A 2011: 711-723.

[26]. V. Krishnakumar, N. Prabavathi, S. Muthunatesan, Spectrochim. Acta 70A (2008) 991-996.

[27]. N. Sundaraganesan, S. Ilakiamani, H. Saleem, P.M. Wojieehowski, D. Michalska, Spectrochim. Acta 61A (2005) 2995-3001.

[28]. D.N. Sathyanarayana, Vibrational Spectroscopy Theory and Application, second ed., New Age International (P) Limited Publishers, New Delhi, 2004.

[29]. S. George, Infrared and Raman Characteristics Group Frequencies Tables and Charts, third ed., Wiley, Chichester, 2001.

[30]. V. Balachandran, K. Parimala, Spectrochim. Acta 102A 2013: 30-51.

[31]. R.A. Kanna Rao, N. Syam Sunder, Spectrochim. Acta 49A 1993: 1691-1699.

[32]. J. Mohan, Organic Spectroscopy Principles and Applications, Narosa Publishing House, New Delhi, 2000.

[33]. Y. Erdogdu, M. Tahir Gulluoglu, M. Kurt, J. Raman Spectrosc. 40 2009: 1615-1623.

[34]. N.F. Chamberlain, The Practice of NMR Spectroscopy with Spectra Structure Correlations for Hydrogen-1, Plenum Press, 1974.

[35]. H.E. Gottlieb, V. kotlyar, A. Nudelman, J. Org. Chem. 62 1997: 7512-7515.

[36]. I. Fleming, Frontier Orbitals and Organic Chemical Reactions, John Wiley and Sons, New York, 1976: pp. 5-27.